NIH Public Access
Author Manuscript
Science. Author manuscript; available in PMC 2009 November 23.

Published in final edited form as:
Science. 2009 January 23; 323(5913): 530–533. doi:10.1126/science.1165740.

Rapid Membrane Disruption by a Perforin-Like Protein Facilitates Parasite Exit from Host Cells

Björn F.C. Kafsack[1,2], **Janethe D. O. Pena**[3], **Isabelle Coppens**[2], **Sandeep Ravindran**[4], **John C. Boothroyd**[4], and **Vern B. Carruthers**[1,*]

1 *Department of Microbiology and Immunology, University of Michigan Medical School, Ann Arbor, MI 48109, USA*

2 *Department of Molecular Microbiology and Immunology, Johns Hopkins Bloomberg School of Public Health, USA*

3 *Department of Immunology, Universidade Federal de Uberlandia, Uberlandia, Brazil*

4 *Department of Microbiology and Immunology, Stanford University School of Medicine, Stanford, CA 94305, USA*

Abstract

Perforin-like proteins are expressed by many bacterial and protozoan pathogens, yet little is known about their function or mode of action. Here we describe TgPLP1, a secreted perforin-like protein of the intracellular protozoan pathogen *Toxoplasma gondii* that displays structural features necessary for pore-formation. Following intracellular growth, TgPLP1-deficient parasites failed to exit normally, resulting in entrapment within host cells. We show that this defect is due to an inability to permeabilize rapidly the parasitophorous vacuole membrane and host plasma membrane during exit. TgPLP1 ablation had little effect on growth in culture, but resulted in a >5-order of magnitude reduction of acute virulence in mice. Perforin-like proteins from other intracellular pathogens may play a similar role in microbial egress and virulence.

Perforin (PF) and members of the membrane attack complex (MAC; complement proteins C6–9) are pore-forming proteins of the innate and adaptive immune response that constitute the founding members of the MACPF domain family (1). Recent studies (2,3) have suggested a shared mechanism of pore formation between the MACPF domain and cholesterol-dependent cytolysins, important virulence factors of many pathogenic bacteria (4).

Perforin-like proteins (PLPs) are found in the genomes of bacterial (5,6) and protozoan pathogens (7,fig. S1), including the intracellular parasite *Toxoplasma gondii. Toxoplasma* causes congenital birth defects, ocular disease, and life-threatening encephalitis in immunocompromised individuals (8). It also serves as a model of other parasites in the phylum Apicomplexa (9) that cause important human diseases such as malaria. Despite their expression by many pathogens, no mode of action or pore-forming activity has been demonstrated for any microbial PLP. Here we show that a *Toxoplasma* perforin-like protein (TgPLP1) aids parasite egress by rapidly compromising the integrity of membranes encasing the parasite.

MACPF domain proteins of the mammalian immune system induce cell death by oligomerizing on the surface of target cells and inserting to form large (~100Å diameter) pores (10). The

*To whom correspondence should be addressed. Email: vcarruth@umich.edu.

Supporting Online Material
www.sciencemag.org, Materials and Methods, Figures S1–S6, Movies S7–S13, References

NIH-PA Author Manuscript
NIH-PA Author Manuscript
NIH-PA Author Manuscript

NIH-PA Author Manuscript

NIH-PA Author Manuscript

NIH-PA Author Manuscript

MACPF domain of TgPLP1 exhibits the core sequence elements important for pore formation including a high degree of similarity to mammalian, bacterial, and protozoan MACPF domains, and the signature (Y/W)-X_6-(F/Y)GTH(F/Y)-X_6-GG motif (fig. S2). Also, structural homology modeling of the TgPLP1 MACPF domain predicts an exquisite preservation of the MACPF domain fold (fig. S3A). Furthermore, the CH1/CH2 helical clusters (helices C–E and I–J, fig. S3B) have alternating hydrophilic and hydrophobic residues, consistent with ability to convert into amphipathic, membrane-spanning β-hairpins during pore insertion (11,12). Finally, a β-sheet-rich domain occupies the TgPLP1 C-terminus, reminiscent of C-terminal β-rich domains in other MACPF proteins (2,13) that play critical roles in membrane binding (11,14).

TgPLP1 localizes to micronemes (Fig. 1A), which are apical secretory organelles important for parasite gliding motility and invasion, and is secreted in a calcium-dependent manner similar to other microneme proteins (Fig. 1B). Deletion of the *plp1* gene by homologous recombination resulted in the loss of TgPLP1 expression in *plp1ko* (Fig. 1, A and C). TgPLP1 expression was restored, albeit to slightly below normal, in *plp1ko/*PLP1*myc* by transfection with PLP1*myc* cDNA (Fig. 1C). Although a second MACPF gene (*plp2*) is present in the genome, no expression of the encoded protein was detected in proteomic studies (15) or in parasites containing an epitope or fluorescent tag inserted at the endogenous *plp2* locus

In malaria parasites, PLP proteins play a role in traversal of the mosquito midgut epithelium by ookinetes (16,17) and the mammalian hepatic sinusoids by sporozoites (18), but their mode of action remains unclear. Cell traversal by sporozoites results in characteristic wounding of the plasma membrane. However, similar to previous findings (19), no cell wounding by *Toxoplasma* tachyzoites was observed, even at very high (>75:1) multiplicity of infection (fig. S4). Thus TgPLP1 plays a role distinct from the characterized malarial PLPs.

After 48h of growth when parasites normally egress, we noticed spherical structures in *plp1ko* cultures that were absent from WT or *plp1ko*/PLP1*myc* and appeared to contain multiple parasites (Fig. 2A). Parasites were often encased by both the parasitophorous vacuolar membrane (PVM) and the host cell plasma membrane (HPM)(Fig. 2B), suggesting an egress defect.

Indeed, following a two-minute treatment with the calcium ionophore A23187, virtually all WT parasites had egressed from infected host cells, while *plp1ko* parasites remained inside their vacuoles (Fig. 2C–D). For a more detailed view of egress, we determined the kinetics of ionophore-induced exit from infected host cells by video microscopy (Fig. 2E). Thirty hours post-infection WT parasites responded rapidly to ionophore addition by initiating gliding motility (average 1.1 ± 0.7min standard deviation) and exiting from the PV shortly thereafter (1.4 ± 0.7min). In contrast, *plp1ko* displayed substantially delayed and temporally heterogeneous egress (6.3 ± 4.3min), with many failing to egress within the 10min observation time. This defect is not due to a failure to respond to ionophore because *plp1ko* parasites activated calcium-dependent motility within the PV at approximately the same time (1.9 ± 1.3min) as WT parasites. While WT tachyzoites registered little resistance crossing the PVM during egress (movie S7), *plp1ko* parasites often demonstrated vigorous movement within the vacuole, prodding and deforming the limiting membrane (movie S8). Eventual escape appears to be the result of persistent gliding motility. Additionally, during attempted egress some *plp1ko* vacuoles rounded up into spherical structures resembling those seen following 48h of culture (movie S9). The complemented *plp1ko*/PLP1*myc* strain displayed an intermediate phenotype with motility activation (1.5 ± 1.7min) similar to both WT and *plp1ko*, and egress timing (3.2 ± 3.3min) slower than WT, yet significantly faster than *plp1ko*. The failure to restore fully the WT phenotype might be due to the sub-normal TgPLP1 protein levels (Fig. 1B) or possible interference by the C-terminal epitope tag. This *plp1ko* egress phenotype was clearly

NIH-PA Author Manuscript

NIH-PA Author Manuscript

NIH-PA Author Manuscript

distinct from the previously described calcium ionophore-response mutant MBE1.1 (20), which displayed a marked delay in motility activation (7.9 ± 2.8min), but exited the vacuole shortly after becoming motile (8.3 ± 3.4min).

Co-infection of host cells with *plp1ko* and WT parasites also restored normal egress of *plp1ko* (Fig. 2F, movie S10). Following egress of an initial WT vacuole, *plp1ko* parasites egressed from the same infected host cell with an indistinguishable delay as parasites from an additional WT vacuole. No such complementation was seen in adjacent infected cells, suggesting the effect is local (fig. S5). This transfer of egress competency in co-infected cells implies that TgPLP1 can act on both the luminal side of the PVM and the cytoplasmic side of a second vacuole. A specific role of TgPLP1 in this process is supported by the persistent egress delay in cells infected with multiple *plp1ko* vacuoles, even after parasites leaving an initial *plp1ko* vacuole had released micronemal and PV contents into the host cytoplasm.

If TgPLP1 indeed facilitates egress by pore-formation, then its secretion should result in permeabilization of the PVM, and possibly the HPM. To test this, we treated cells at 30h post-infection with cytochalasin D to disable parasite motility, and then induced microneme secretion by ionophore treatment. To detect disruption of the HPM we added the membrane-impermeant nuclear dye propidium iodide (PI) to the medium. After fixation and selective detergent permeabilization of the HPM and PVM, we stained for a soluble PV marker (GRA1) to monitor PVM permeabilization and a microneme protein (SUB1) to detect microneme secretion. These three markers (PI, GRA1, and SUB1) enabled us to discern four distinct permeabilization stages in cells infected by WT parasites.

In stage 0, PI remained excluded from the host cell, GRA1 remained contained within the PV, and no SUB1 staining was observed, indicating that both the HPM and PVM were intact and that micronemes were not secreted (Fig. 3A). Progression to stage 1 was marked by release of microneme proteins onto the parasite surface (see inset) and disruption of the PVM as indicated by GRA1 staining diffusely throughout the host cell, yet the HPM remained intact and continued to exclude PI. By stage 2 the HPM became permeable to PI as indicated by labeling of the host cell nucleus. Nuclear labeling only occurred after GRA1 diffusion from the PV, never before, suggesting an inside-out disruption of the PVM first and the HPM second. The final stage (stage 3) was characterized by diffusion of SUB1 into the host cell cytoplasm.

While PVM permeabilization was often (84.7%) observed in of WT infected cells, it was rarely (8.2%) seen in *plp1ko* infected cells (Fig. 3B). Similarly, HPM permeabilization occurred in 73.0% of WT infected cells and only 3.0% of *plp1ko* infected cells. The *plp1ko*/PLP1*myc* complementation strain showed partial restoration of both GRA1 release from the PV (47.4%) and nuclear labeling (32.2%). Additionally, cells infected with *plp1ko* displayed a unique labeling pattern (Fig 3A, bottom row, second panel) not observed in either WT or *plp1ko*/PLP1*myc*, marked by microneme secretion without concomitant release of the vacuolar contents (stage 1′), again suggesting that TgPLP1 is critical for PVM permeabilization even when other microneme contents have been secreted.

By expressing the soluble fluorescent marker DsRed in the PV, we monitored PVM permeabilization in real-time. After calcium ionophore addition we observed a rapid redistribution of fluorescence from cytochalasin D-immobilized WT and *plp1ko*/PLP1*myc* vacuoles to the host cell cytoplasm (Fig. 3C–D, movie S11–12). No such fluorescence release was ever observed from *plp1ko* vacuoles (Fig 3C–D, movie S13) within the 10min observation window. These findings demonstrate that TgPLP1 is necessary to permit the escape of macromolecules from the PV, and also suggest that mechanical disruption of the PVM by gliding motility rather than a second pore forming activity (e.g., TgPLP2) is responsible for residual egress of *plp1ko*.

NIH-PA Author Manuscript

NIH-PA Author Manuscript

NIH-PA Author Manuscript

While deletion of *plp1* had no apparent effect on in vitro intracellular growth (fig. S6), in vivo studies revealed a >5-order of magnitude attenuation of virulence (Fig. 3E). Mice injected with 10 or more tachyzoites of WT or *plp1ko*/PLP1*myc* generally died within 15 days, but mice infected with up to 1 million *plp1ko* tachyzoites survived to the endpoint.

We propose that pore formation in the PVM weakens this membranous barrier to permit parasite escape and/or acts as a conduit for additional effector proteins that aid in egress. Also, an uncharacterized PLP expressed in malaria blood stage parasites (21) may play a role analogous to TgPLP1 in parasite egress from infected erythrocytes.

Supplementary Material

Refer to Web version on PubMed Central for supplementary material.

References and Notes

1. Voskoboinik I, Smyth MJ, Trapani JA. Nat Rev Immunol 2006;6:940. [PubMed: 17124515]
2. Rosado CJ, et al. Science 2007;317:1548. [PubMed: 17717151]
3. Hadders MA, Beringer DX, Gros P. Science 2007;317:1552. [PubMed: 17872444]
4. Tweten RK. Infect Immun 2005;73:6199. [PubMed: 16177291]
5. Ponting CP. Curr Biol 1999;9:R911. [PubMed: 10608922]
6. Rosado CJ, et al. Cell Microbiol 2008;10
7. Kaiser K, et al. Mol Biochem Parasitol 2004;133:15. [PubMed: 14668008]
8. Montoya JG, Liesenfeld O. Lancet 2004;363:1965. [PubMed: 15194258]
9. Kim K, Weiss LM. Int J Parasitol 2004;34:423. [PubMed: 15003501]
10. Pipkin ME, Lieberman J. Curr Opin Immunol 2007;19:301. [PubMed: 17433871]
11. Shatursky O, et al. Cell 1999;99:293. [PubMed: 10555145]
12. Tilley SJ, Saibil HR. Curr Opin Struct Biol 2006;16:230. [PubMed: 16563740]
13. Sutton RB, et al. Cell 1995;80:929. [PubMed: 7697723]
14. Li JD, Carroll J, Ellar DJ. Nature 1991;353:815. [PubMed: 1658659]
15. http://toxodb.org/toxo/showRecord.do?name=GeneRecordClasses.GeneRecordClass&project_id=ToxoDB&primary_key=5
16. Ishino T, Chinzei Y, Yuda M. Cell Microbiol 2005;7:199. [PubMed: 15659064]
17. Ecker A, et al. Exp Parasitol 2007;116:504. [PubMed: 17367780]
18. Kadota K, et al. Proc Natl Acad Sci U S A 2004;101:16310. [PubMed: 15520375]
19. Mota MM, et al. Science 2001;291:141. [PubMed: 11141568]
20. Black M, Arrizabalaga G, Boothroyd J. Mol Cell Bio 2000;20:9399. [PubMed: 11094090]
21. Florens L, et al. Nature 2002;419:520. [PubMed: 12368866]

22. We thank T. Schultz, S. Meshinchi, A. Silva, E. Mastrantonio and C. Pereira for technical assistance; D. Roos and F. Dzierszinski for reagents; G. Zeiner for help with the HA-tagging; and M.-H. Huynh, L.D. Sibley, J. Swanson, and M. O'Riordan for valuable discussion and input. This work was supported by NIH RO1 AI46675 and a pre-doctoral fellowship by the American Heart Association. TgPLP1 Genbank accession number is EF102772.

NIH-PA Author Manuscript

NIH-PA Author Manuscript

NIH-PA Author Manuscript

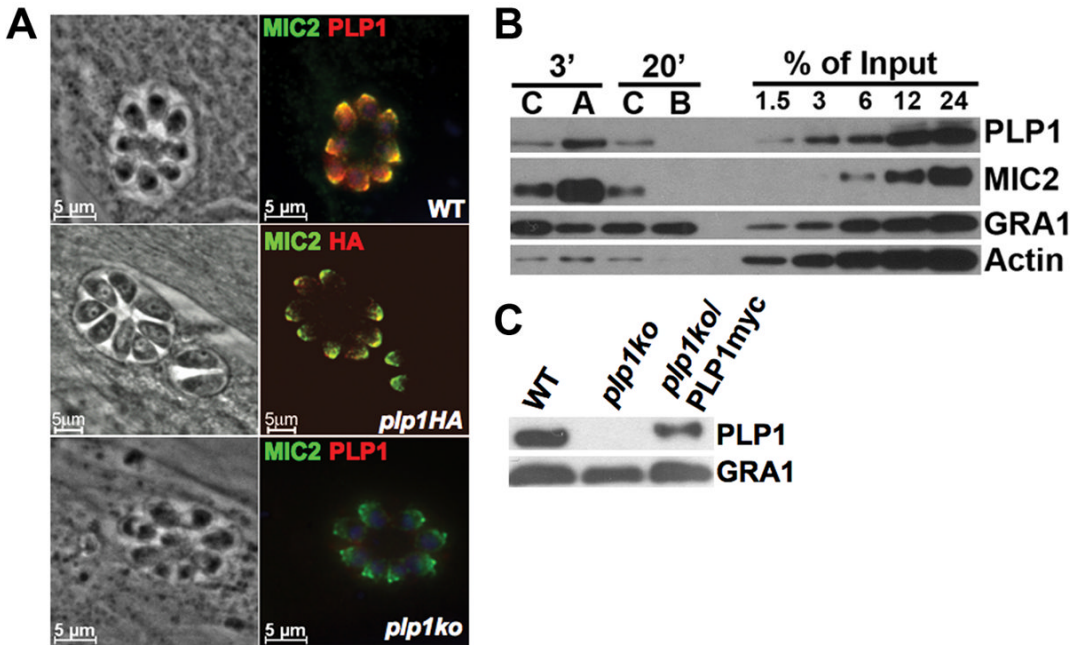

Figure 1.

TgPLP1 is secreted from the micronemes in a calcium-dependent manner. **(A)** Immuno-localization of TgPLP1 (red) and the microneme marker MIC2 (green) in WT, epitope-tagged *plp1HA*, and *plp1ko* strains. **(B)** Secretion of TgPLP1, MIC2, and constitutively secreted GRA1 in response to a 3min treatment with the calcium ionophore A23187 (A), 20min with the calcium chelator BAPTA-AM (B), or appropriate solvent control (C). Actin included as control for inadvertent lysis. **(C)** Immunoblot of TgPLP1 in WT, *plp1ko*, and *plp1ko*/PLP1*myc* strains.

NIH-PA Author Manuscript
NIH-PA Author Manuscript
NIH-PA Author Manuscript

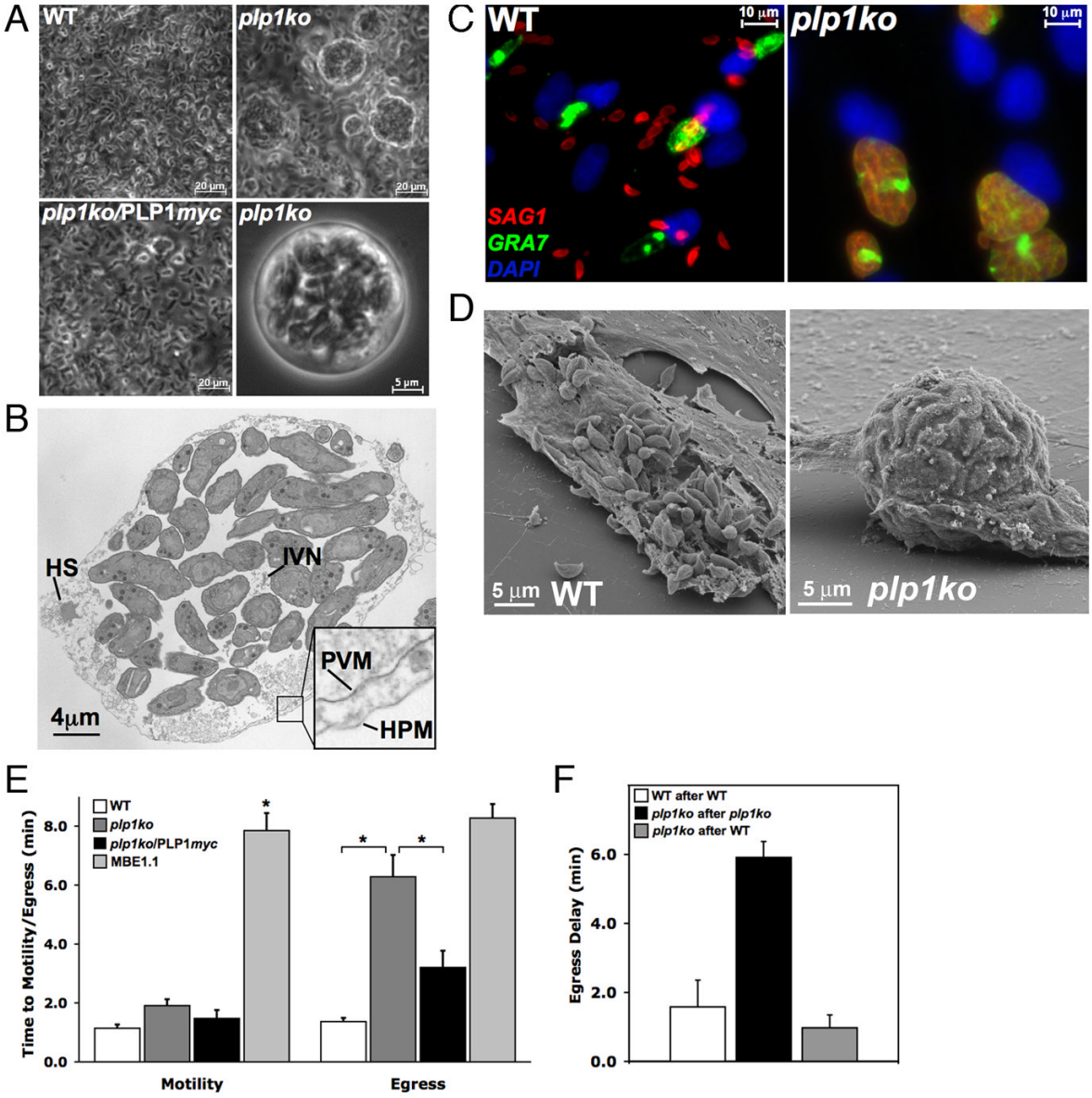

Figure 2.

plp1ko egress phenotypes (**A)** Parasite cultures 48h post-infection. **(B)** Transmission electron micrograph of spherical structures shows remnants of host cell structures (HS), the intravacuolar network (IVN), and numerous tachyzoites encased by the parasitophorous vacuolar membrane (PVM) and host cell plasma membrane (HPM). **(C–D)** Ionophore-induced egress from WT or *plp1ko* vacuoles. IFA colors: Parasites, red; PVM, green; host nuclei, blue. **(E)** Time to motility activation or egress following addition of calcium ionophore in WT, *plp1ko*, *plp1ko*/PLP1*myc*, and MBE1.1. Error bars are SEM ($n \geq 30$) and asterisk indicates $P < 0.05$ (Student's t-test). **(F)** Egress delay of secondary vacuoles following egress of an initial vacuole from cells multiply-infected with WT, *plp1ko*, or both.

NIH-PA Author Manuscript

NIH-PA Author Manuscript

NIH-PA Author Manuscript

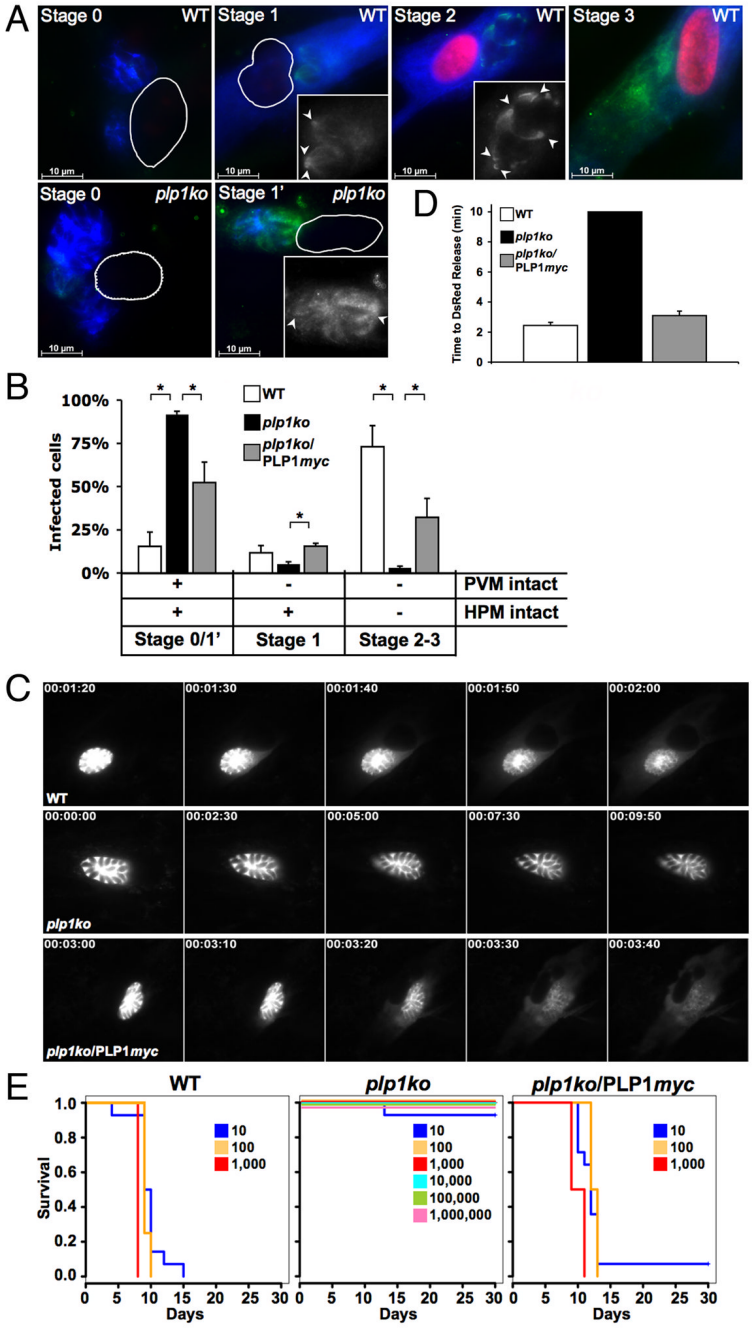

Figure 3.

Evidence of pore formation by TgPLP1 **(A)** Ionophore-induced permeabilization by immobilized WT or *plp1ko* tachyzoites. Stage 0: PV marker (GRA1, blue) remains contained within the PVM, no microneme release (SUB1, green), no labeling of host cell nucleus by PI, (red or outlined when unlabeled). Stage 1: Microneme contents have been secreted onto the parasite surface (green, see also inset; arrowhead = parasite apex), PV markers have diffused throughout the host cell but host cell nucleus remains unlabeled. Stage 2: Host nucleus is now PI positive, indicating permeabilization of the HPM. Stage 3: Microneme proteins have diffused throughout the host cytoplasm. Cells infected by *plp1ko* remain in stage 0 or display microneme secretion without PV marker release (stage 1′). **(B)** Quantification of induced PVM

NIH-PA Author Manuscript

NIH-PA Author Manuscript

NIH-PA Author Manuscript

and HPM permeabilization for WT, *plp1ko*, or *plp1ko*/PLP1*myc*. Error bars are SEM ($n = 6$) and asterisk indicates $P < 0.05$ (Student's t-test). **(C)** Rapid release of DsRed from the vacuole in WT (top) and *plp1ko*/PLP1*myc* (bottom), but not *plp1ko* (middle). Time stamp (h:min:sec) indicates time following calcium ionophore addition. **(D)** Average time to DsRed release within a 10min observation period. Error bars are SEM ($n \geq 30$). **(E)** Virulence in outbred mice following inoculation of escalating tachyzoite numbers.